DOI: 10.1002/cbic.200700468

Affinity Analyses on Moldable Optical Polycarbonate

Kwang-Seuk Ko, Peyman Najmabadi, James J. La Clair,* and Michael D. Burkart*[a]

The integration of molecular analyses within modern media requires a general approach to display molecular receptors in three-dimensional space. Current methods include the use of assemblies of beads (Figure 1A),[1] lithography or nanolithography to generate surface microarrays (Figure 1B),[2] or self-assembly processes (Figure 1C).[3] Here we investigate the development of arrays by directly molding receptors in plastic (Figure 1D). This approach offers versatility in the fabrication of biosensors for both two- and three-dimensional arrays.

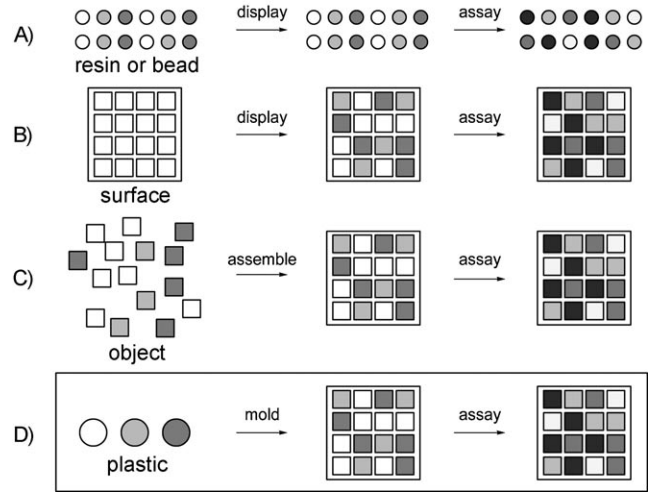

Figure 1. Strategies for constructing and actualizing affinity based devices. A) Bead-based methods use sorting to generate, display, and analyze molecular reactions. B) Lithographic methods are implemented to display surface microarrays and transact analyses on their surface. C) Self-assembled devices can also be used to develop microarrays. D) Molding of plastics can also be implemented to display receptor arrays.

To develop this process, we turned to polycarbonate (PC), as its superior mechanical and optical properties have led to its general use in laboratory and clinical devices.[4] PC is a thermoplastic polymer that is highly transparent to visible light and provides better optical properties than many types of glasses as well as high impact (Hardness–Rockwell M70) and temperature resistance ($<130\,^{\circ}C$).[5] Most importantly, it can be molded on a commercial scale by using injection molding and extrusion methods.[6]

We began by designing a general strategy to dope receptors in PC. A motif was required that was soluble in PC, yet would not be extracted when exposed to aqueous media. Compound **1** was chosen as it contained a tricarbonate tail for retention in PC (left-hand boxes in Figure 2A), a polyethylene glycol linkage to deliver the receptor to the surface (center boxes in Figure 2A), and an amide bond for ligand attachment (right-hand boxes in Figure 2A). Moreover, spectrophotometric analysis substantiated a better doping efficacy when using compound **1** in comparison with **2** and **3**, as shown in Figure 2B. This analysis was performed in order to determine the relative doping efficacy. Milled polycarbonate 100–200 μm resin was doped from solutions containing 100, 50, 5, 0.5, or 0.1 nM of **1**–**3**. Solutions were filtered after the doping process and analyzed spectrophotometrically for the uptake of **1**–**3** in the resin. The relative uptake was best observed from 0.1 nM of **1**–**3**. Figure 2B depicts the relative fluorescence intensity of solutions. As shown, compound **1** provides the best doping efficacy.

The synthesis of dopant **1** was completed in six steps from commercially available bisphenol A (**4**). The synthesis was begun by applying the methods of Brunelle[7] to prepare oligomer **5**. Under high dilution, **5** was converted to **6** by sequential treatment with methylchloroformate and *p*-nitrophenylchloroformate. The desired poly(ethylene glycol) linkage was then installed by coupling **6** to single-molecular-weight azidopoly(ethylene glycol) **7** to afford **8** (see Scheme 1 and the Supporting Information).

A fluorescent sandwich assay with a murine monoclonal antibody (mAb) XRI-TF35,[8] elicited against the 7-dimethylaminocoumarinacetamide motif, was used to evaluate receptors arrays developed from **8**. For this antibody, receptor-labeled **1** was prepared by Staudinger reduction of azide **8** followed by peptide coupling to acid **9** (Scheme 1). As designed, the left side of **1** served to anchor the material in PC, and the right side provided a ligand to screen surface accessibility.

Doping studies were conducted on commercially-available Makrolon CD2005 PC milled to 150 ± 50 μm and doped by shaking 100 mg of resin in 1 mL of 50 nM **1** in ethanol for 2 h, followed by washing with water or phosphate-buffered saline (PBS). This protocol was sufficient to prepare resins doped with standardized concentrations to the limit of detection of **1** by fluorescence microscopy (~10 nM on Nikon TE 3000 at maximum excitation at 377 ± 50 nm and emission at 447 ± 60 nm).

The effectiveness of the doping process was evaluated by screening samples of the doped PC for leaching of **1**. After weeks of incubation in PBS, no significant changes were observed in the intensity of blue light emission from resin doped with 50 nM **1** (see the Supporting Information) or by examining the aqueous media spectrophotometrically.

[a] *Dr. K.-S. Ko, Dr. P. Najmabadi, Dr. J. J. La Clair, Prof. Dr. M. D. Burkart*
Department of Chemistry and Biochemistry
University of California–San Diego
9500 Gilman Drive, La Jolla, CA 92037-0358 (USA)
Fax: (+1) 858-822-2182
E-mail: mburkart@ucsd.edu
jlaclair@ucsd.edu

Supporting information for this article is available on the WWW under http://www.chembiochem.org or from the author.

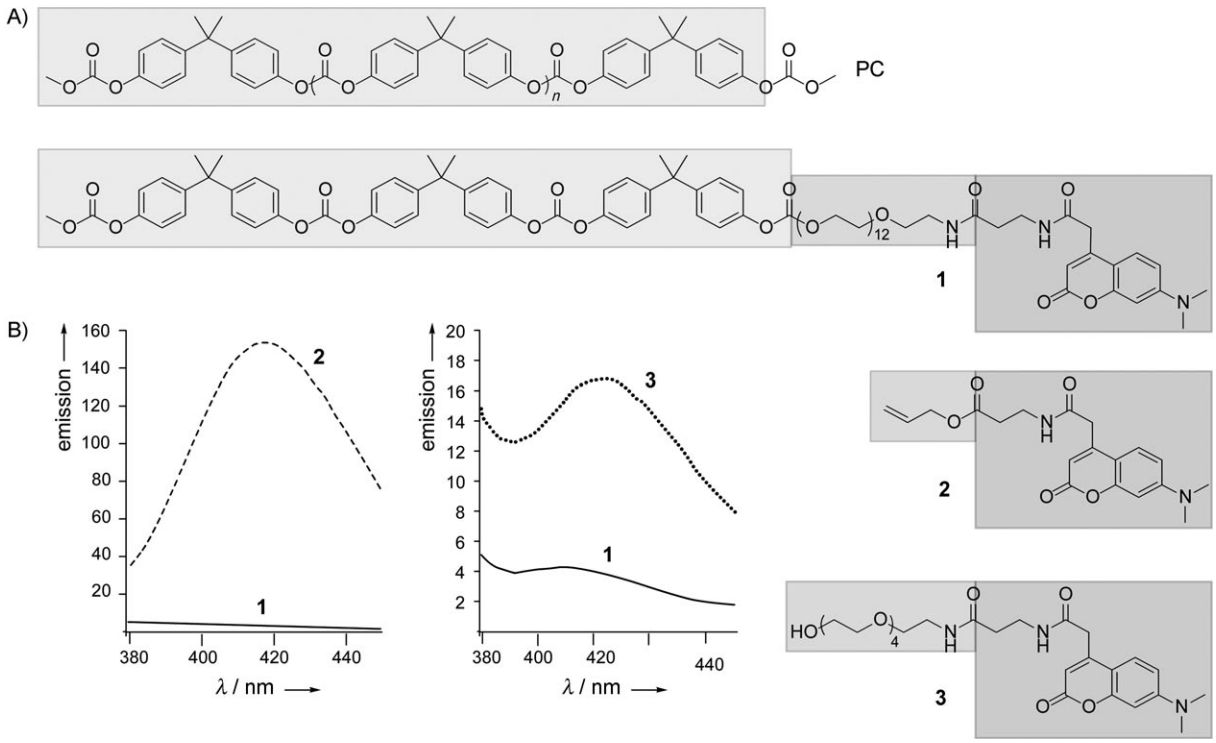

Figure 2. A) Structures of polycarbonate (PC) and dopant **1** and fluorescent labels **2** and **3**. Boxed regions denote function as given by a PC solubilizing anchor (left), linker (center), and receptor (right), *n* denotes the number of ethylene glycol units. B) Spectrophotometric analysis depicts the amount of ligand remaining in the mother liquor after doping 1.0 g of resin with substrate in ethanol (50 nM, 2.0 mL). These plots display the emission scanned at 1 nm resolution from 380–450 nm under a constant excitation at 350 nm. The ligands **1**–**3** were taken up in the order of **1** > **3** ≫ **2**.

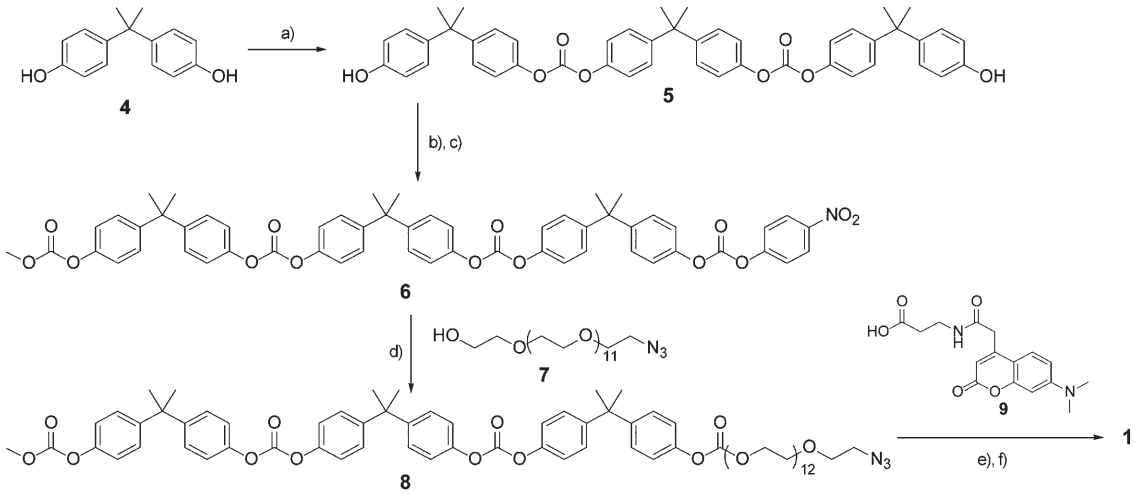

Scheme 1. Synthesis of dopant **1**. Reagents and conditions: a) i: *tert*-butyl dimethyl silyl chloride, Et_3N, *N*,*N*-dimethylformamide (DMF), RT; ii: 4-nitrophenylchloroformate, Et_3N, THF, 0 °C; iii: **4**, Et_3N, THF, 0 °C; iv: tetrabutylammonium fluoride, THF, 73% over four steps. b) MeOCOCl, Et_3N, THF, 0 °C to RT, 1.5 h, 83%. c) *p*-nitrophenylchloroformate, Et_3N, CH_2Cl_2, 30 min, 96%. d) Et_3N, CH_2Cl_2, 2 h, 88%. e) H_2, Pd/C, MeOH, CH_2Cl_2, 12 h, 88%. f) 1-ethyl-3-(3-dimethylaminopropyl)-carbodiimide hydrochloride, 1-hydroxybenzotriazole, DMF, RT, 8 h, 65%.

The molecular affinity of the resin was determined prior to molding by using a dual-color fluorescent antibody sandwich assay. The experiment was designed such that **1** was analyzed by using a blue fluorescent channel (Figure 3A). This resin was then treated with aliquots of the XRI-TF35- and FITC-labeled anti-mouse antibodies each examined at 3 nM, 30 nM, 0.3 μM, and 3 μM. Fluorescence from binding of the XRI-TF35 mAb was determined by hybridization of an equivalent amount of secondary FITC-labeled anti-mouse IgG (Figure 3C). Compared to the control resin, **g1**, a concentration-dependent binding event was observed as given by an increase in green fluorescence light intensity compared to the concentration of XRI-TF35 mAb (**g2**–**g5**, Figure 3C). The DMC **1**-doped polycarbonate granules that are not treated with either primary or

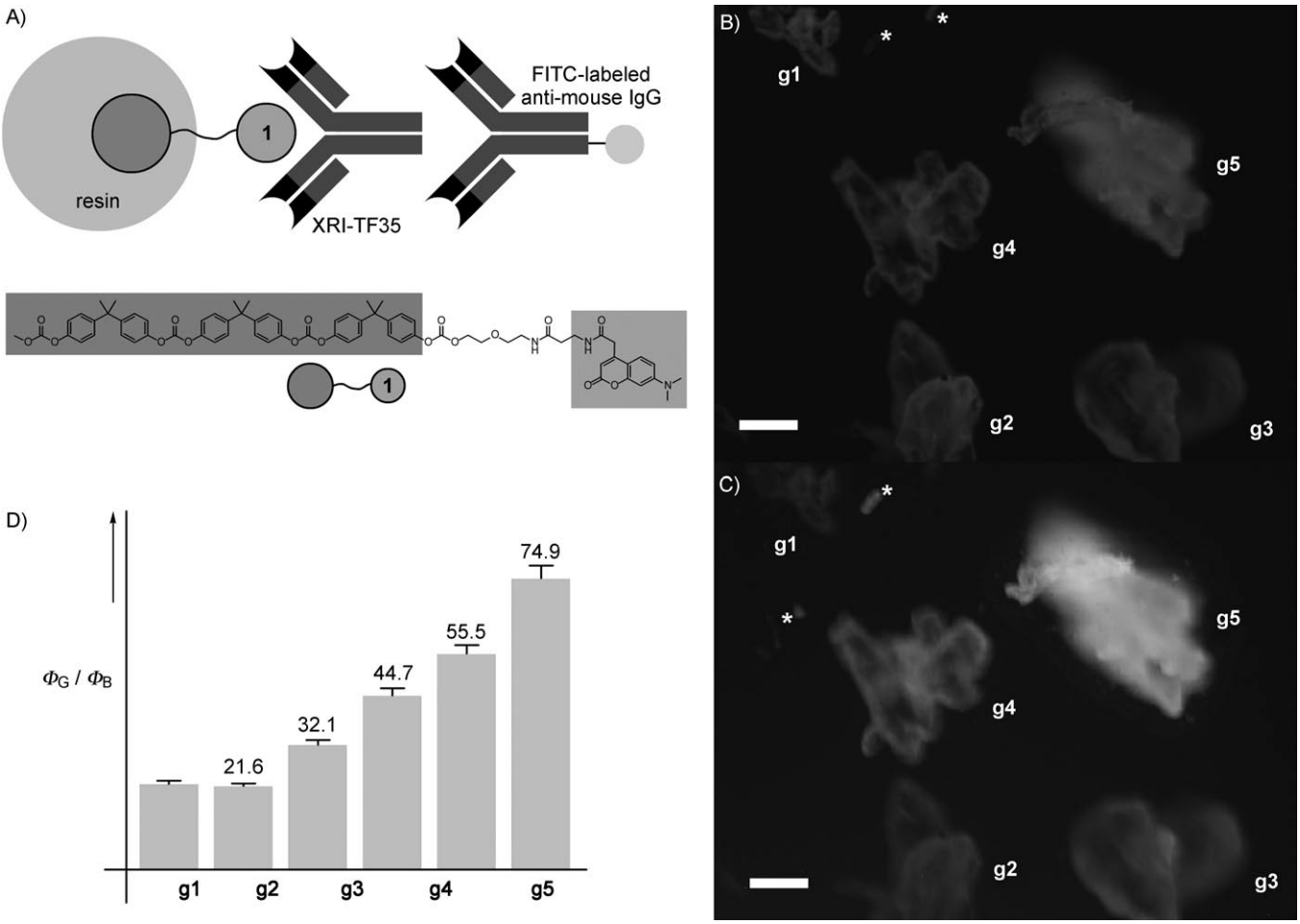

Figure 3. Polycarbonate resin-based, antibody-based sandwich assay. A) Dual-color fluorescent analysis on doped PC resins depicting the binding of a primary XRI-TF35 mAb to the 7-dimethylaminocoumarin-acetamide label in resin-bound **1**. The affinity event was visualized by examining the complexation of a secondary FITC-labeled anti-mouse IgG mAb. B) Fluorescent image collected with excitation at 377 ± 50 nm and emission at 447 ± 60 nm of five resins by using a BrightLine DAPI-5060B filter set. **g1** denotes a granule doped with 50 nM **1** that was not treated with the XRI-TF35 primary mAb. **g2**–**g5** denote granules doped with 50 nM **1** and treated with various concentrations of primary mAb and secondary FITC-labeled anti-mouse IgG mAb. The concentration of the primary mAb was given by 3 nM in **g2**, 30 nM in **g3**, 0.3 μM in **g4**, and 3 μM in **g5**. The mAb was also treated with the same amounts of secondary FITC-labeled anti-mouse IgG. C) Fluorescent image of the same resins as in (B) collected with excitation at 500 ± 24 nm and emission 542 ± 27 nm by using a BrightLine YFP-2427A filter set. An asterisk denotes inadvertent fluorescent debris arising during the transfer of resin to the glass slide. Scale bars = 100 μm. D) A plot depicting the relative fluorescence at different wavelengths for each resin **g1**–**g5**.

secondary antibodies act as the control, **g1**. The small amount of green fluorescence observed from **g1** in Figure 3C arises from inherent background fluorescence observed in polycarbonate. A comparable background was also obtained in resin that was not doped with **1**. This intensity did not increase at the limit detection by fluorescence microscopy when the doped resin was treated with FITC-labeled anti-mouse IgG (concentrations < 30 μM were screened).

We then quantitatively evaluated the assay by using two-color fluorescent imaging. The fluorescent intensity of samples shown in Figure 3B and C was sampled from regions of each resin by using ImageJ.[9] Five random locations in each of the resins depicted in Figure 3B were recorded by using a rectangle of 20×20 pixels. This procedure was repeated for the green fluorescent image (Figure 3C) with an identically sized rectangle and identical positioning. Then, the mean value of the five points was calculated for each of the samples as well as for the background. The relative green-to-blue intensity, as depicted in Figure 3D, confirmed the concentration dependency of this assay.

With the assay established on resin format, we turned our attention to using resin **g5** to mold objects containing small regions of the reporter **1**. Samples of the granules in **g5** were sprinkled on the top of a cylindrical mold loaded with PC and pressed to form a lens (see the Supporting Information). Upon repeating the dual-color fluorescent analysis, regions that appeared on the surface of the lens (**g5***, Figure 4) reacted positively to the binding of the green fluorescent antibody complex, while regions within the PC (**g5**, Figure 4) did not uptake the antibody complex. The entire lens pressing and analysis

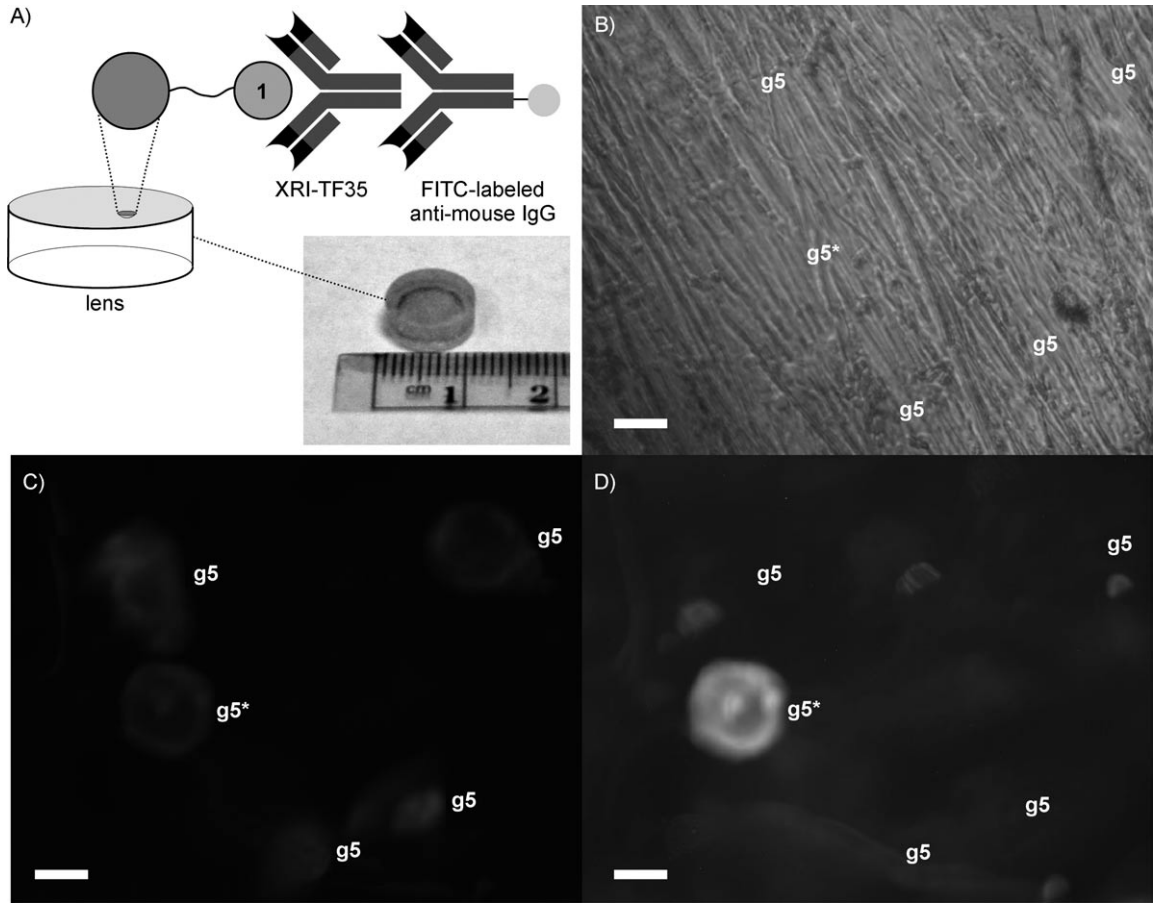

Figure 4. Antibody-based sandwich analysis conducted on the surface of a molded PC lens. A) An illustration of the sandwich assay and a photograph of the lens. This assay was conducted under identical conditions to those given in Figure 3. B) A white-light image depicting the surface of the lens. Molding (see the Supporting Information) supplies a transparent surface with receptors from individual granules available at the surface for microarrays or affinity-based assays. This surface contained imperfections at the 10–30 μm level, as the surface was used directly from the molding process without polishing. C) Blue fluorescence from regions in (B) collected with excitation at 377 ± 50 nm and emission at 447 ± 60 nm from five resins by using a BrightLine® DAPI-5060B filter set. The regions of blue fluorescence denote the position of **1** localized on the lens as delivered from **g5** granules prior to melting. D) Green fluorescence from regions in (B) in which the surface was treated with 3 μM XRI-TF35 and 3 μM FITC-labeled anti-mouse IgG antibodies. Green fluorescence arises from the binding of FITC-labeled mAb complex to the receptor regions on the surface and was collected with excitation at 500 ± 24 nm and emission 542 ± 27 nm by using a BrightLine® YFP-2427A filter set. **g5*** denotes doped regions exposed to surface and **g5** denotes regions molded inside the PC. Fluorescence was collected as stated in Figure 3. Scale bars = 100 μm.

process was repeated three times with deviations in the intensity of spots on the surface of within 5% when prepared by hand. This deviation can be profoundly reduced upon automation, as already established for a wide range of mass-produced polycarbonate objects, including compact discs.[5]

These experiments now provide a means to engineer active receptor arrays on three-dimensional polycarbonate objects by using conventional thermal molding. The method is practical and requires minimal cost and effort to design and implement. This method, as illustrated by the pressing of a lens in Figure 4, can be used to manufacture optical devices containing patterns of fluorescent materials or reporters for subsequent analyses. Such components can provide an affordable means to allow optical components to become part of an analytical system. Efforts are underway to deliver optimized systems with reactive labels to attach and screen biologically relevant affinity events.

Acknowledgement

This work was supported by the NSF grant BES-0520868. We thank Jordan Meier for developing the procedure for milling the PC resin used in this experimentation and Bayer Material Science for a sample of the PC used.

Keywords: assays · microarrays · polycarbonates · polymers · proteins

[1] R. C. Summerbell, C. A. Levesque, K. A. Seifert, M. Bovers, J. W. Fell, M. R. Diaz, T. Boekhout, G. S. de Hoog, J. Stalpers, P. W. Crous, *Philos. Trans. R. Soc. London Ser. B* **2005**, *360*, 1897–1903.
[2] A. A. Tseng, A. Notargiacomo, *J. Nanosci. Nanotechnol.* **2005**, *5*, 683–702.
[3] a) W. Senaratne, P. Sengupta, V. Jakubek, D. Holowka, C. K. Ober, B. Baird, *J. Am. Chem. Soc.* **2006**, *128*, 5594–5595; b) B. P. Corgier, A. Laurent, P. Perriat, L. J. Blum, C. A. Marquette, *Angew. Chem.* **2007**, *119*, 4186–4188; *Angew. Chem. Int. Ed.* **2007**, *46*, 4108–4110; c) M. J. W. Ludden, A. Mulder,

R. Tampé, D. N. Reinhoudt, J. Huskens, *Angew. Chem.* **2007**, *119*, 4182–4185; *Angew. Chem. Int. Ed.* **2007**, *46*, 4104–4107.

[4] a) H. Becker, L. E. Locascio, *Talanta* **2002**, *56*, 267–287; b) J. J. La Clair, M. D. Burkart, *Org. Biol. Chem.* **2003**, *1*, 3244–3249; c) J. J. La Clair, M. D. Burkart, *Org. Biol. Chem.* **2006**, *4*, 3052–3055; d) H. Kido, A. Maquieira, B. D. Hammock, *Anal. Chim. Acta* **2000**, *411*, 1–11; e) I. Alexandre, Y. Houbion, J. Collet, S. Hamels, J. Demarteau, J. L. Gala, J. Remacle, *BioTechniques* **2002**, *33*, 435–439; f) O. Carion, V. Souplet, C. Olivier, C. Maillet, N. Medard, O. El-Mahdi, J.-O. Durand, O. Melnyk, *ChemBioChem* **2007**, *8*, 315–322; g) Y. Liu, C. B. Rauch, *Anal. Biochem.* **2003**, *317*, 76–84; h) S. A. Soper, M. Hashimoto, C. Situma, M. C. Murphy, R. L. McCarley, Y. W. Cheng, F. Barany, *Methods* **2005**, *37*, 103–113; i) U. Bora, P. Sharma, S. Kumar, K. Kannan, P. Nahar, *Talanta* **2006**, *70*, 624–629; j) S. Suye, Y. Kumon, A. Ishigaki, *Biotechnol. Appl. Biochem.* **1998**, *27*, 245–248; k) Y. Li, Z. Wang, L. M. L. Ou, H. Z. Yu, *Anal. Chem.* **2007**, *79*, 426–433.

[5] K. C. Polmann, *The Compact Disc Handbook*, A–R Editions, Madison, **1992**.

[6] R. J. Crawford, *Plastic Engineering*, 2nd ed., Pergamon, Oxford, **1987**.

[7] D. J. Brunelle, T. G. Shannon, *Macromolecules* **1991**, *24*, 3035–3044.

[8] The XRI-TF5 mAb was obtained as a gift from the Xenobe Research Institute, San Diego, CA. This mouse mAb displayed a $K_d = 0.62 \pm 0.08$ nM to *N*,*N*-dimethyl-7-dimethylaminocoumarin-4-acetamide, as established by using microequlibrium dialysis (Harvard Biosciences, Holliston, MA). The use of this antibody was described in: C. J. Forsyth, L. Ying, J. Chen, J. J. La Clair, *J. Am. Chem. Soc.* **2006**, *128*, 3858–3859.

[9] ImageJ is a Java-based image-processing tool developed at the National Institutes of Health see: http://rsb.info.nih.gov/ij/. For applications or related publications see: a) R. Carmona, D. Macías, J. A. Guadix, V. Portillo, J. M. Pérez-Pomares, R. Muñoz-Chápuli, *J. Microsc.* **2007**, *225*, 96–99; b) R. Cathelin, F. Lopez, C. Klopp, *Bioinformatics* **2007**, *23*, 247–248.

Received: May 21, 2007
Revised: October 9, 2007
Published online on December 20, 2007

